Chemical Physics Letters 464 (2008) 211–215

Contents lists available at ScienceDirect

Chemical Physics Letters

journal homepage: www.elsevier.com/locate/cplett

Femtosecond nonlinear optical properties of alkoxy phthalocyanines at 800 nm studied using Z-Scan technique

N. Venkatram [a], D. Narayana Rao [a], L. Giribabu [b], S. Venugopal Rao [c,*]

[a] School of Physics, University of Hyderabad, Hyderabad 500 046, Andhra Pradesh, India
[b] Nanomaterials Laboratory, Inorganic & Physical Chemistry Division, Indian Institute of Chemical Technology, Hyderabad 500 007, Andhra Pradesh, India
[c] Advanced Centre of Research on High Energy Materials (ACRHEM), University of Hyderabad, Hyderabad 500 046, Andhra Pradesh, India

ARTICLE INFO

Article history:
Received 7 August 2008
In final form 15 September 2008
Available online 19 September 2008

ABSTRACT

We report our results on the nonlinear absorption, and its switching behavior, of two alkoxy phthalocyanines (a) 2,3,9,10,16,17,23,24-octakis-(heptyloxy) phthalocyanine (Pc1) and (b) 2,3,9,10,16,17,23,24-octakis-(heptyloxy) phthalocyanine zinc(II) (Pc2) studied at a wavelength of 800 nm with ~100 fs pulses using the standard Z-scan technique. Both the molecules possessed negative nonlinear refractive index (n_2) as revealed by signature of the closed aperture data. Magnitudes of the n_2 evaluated were $\sim 1.26 \times 10^{-13}$ esu for Pc1 and $\sim 1.68 \times 10^{-13}$ esu for Pc2. Nonlinear absorption data of Pc1 obtained at a concentration of 5×10^{-4} M demonstrated complex behavior with switching from reverse saturable absorption (RSA) within saturable absorption (SA) at low peak intensities to SA in RSA at higher peak intensities. Pc2 data recorded at similar concentration exhibited saturable absorption type of behavior at lower peak intensities. The nonlinear absorption at higher intensities was again multifarious with switching over from SA to RSA. We discuss the complicated behavior of the nonlinear absorption and nonlinear optical performance of these molecules for their potential applications.

1. Introduction

Phthalocyanines and porphyrins besides their metal derivatives are macromolecules with large number of delocalized π electrons possessing interesting third-order nonlinear optical (NLO) properties with prominent applications in optical limiting and all-optical switching [1–21]. The capability of phthalocyanine macromolecule to accommodate different metal ions in their cavity has ramification in diverse optical properties [3–8]. For organic materials, in general, the real part of the nonlinear optical susceptibility which is a manifestation of the nonlinear refractive index facilitates all-optical switching in picosecond/sub-picosecond time scales whereas the imaginary part, result of nonlinear absorption, augments the most popular optical limiting mechanism with nanosecond pulses. Interestingly, molecules with large two-photon and three-photon absorption cross-sections have remarkable potential in imaging and lithographic applications [22]. Phthalocyanines are versatile molecules possessing the above properties in the visible and near-infrared spectral region. The finest optical limiting performance for any organic molecule in the nanosecond domain was achieved using a phthalocyanine [23] justifying the potential of these molecules. Although NLO properties of numerous phthalocyanines and their derivatives have been investigated until date [3–21] there is further scope for discovering novel structures with advanced figures of merit, specifically, with ultrafast refractive nonlinearities and multi-photon absorption coefficients. An iterative process of novel molecule synthesis followed by nonlinear properties testing, exploring, and optimizing the structure–property relationship to improve the molecules is vital for recognition of materials with actual device potential.

Recently we have synthesized and studied the NLO properties of alkyl and alkoxy phthalocyanines in femtosecond, nanosecond, and continuous wave domains [9–13]. Alkyl phthalocyanines studied with femtosecond pulses revealed strong three-photon absorption near 800 nm [9,10]. The molecules used in this study were investigated earlier with nanosecond pulses and we measured strong nonlinear absorption as well as the overall nonlinearity [11]. Continuous wave NLO studies also suggest strong optical limiting behavior with low limiting thresholds [12,13]. However, the performance in the femtosecond (fs) domain will be important for the absolute evaluation of device potential. We report here our results on the femtosecond NLO properties of two alkoxy phthalocyanines [2,3,9,10,16,17,23,24-octakis-(heptyloxy) phthalocyanine and 2,3,9,10,16,17,23,24-octakis-(heptyloxy) phthalocyanine zinc(II); herewith represented as Pc1 and Pc2, respectively, throughout this Letter] studied using fs pulses at a wavelength of 800 nm with the standard Z-scan technique [24]. The merits of these phthalocyanines comprise (a) planar structure and facile synthesis, (b) easy dissolution in common solvents, and (c) excellent chemical and thermal stability. The sign and magnitude of

* Corresponding author. Fax: +91 040 23012800.
E-mail addresses: dnrsp@uohyd.ernet.in (D. Narayana Rao), svrsp@uohyd.ernet.in (S. Venugopal Rao).

0009-2614/$ - see front matter © 2008 Elsevier B.V. All rights reserved.
doi:10.1016/j.cplett.2008.09.029

nonlinear refractive index were obtained from the closed aperture Z-scan data. From the nonlinear absorption data, achieved through open aperture Z-scans, we derived the two-photon, three-photon, and excited state absorption cross-sections. Our studies in the femtosecond domain provide sufficient evidence that these molecules possess superior nonlinear coefficients required for applications in optical limiting and switching.

2. Experimental details

The samples were synthesized and purified according to the procedures reported in the literature [25]. Each one was subjected to a column chromatographic purification process preceding the measurements. Molecular structures and the absorption spectra of Pc1 and Pc2 are reported elsewhere [9,12]. These molecules show the characteristic linear absorption features typical of other phthalocyanines, the high energy B (Soret) band and the low energy Q band(s). Metal-free phthalocyanine had two peaks in the Q-band while the Zn phthalocyanine had one peak. The experiments were performed with sample solutions dissolved in chloroform and placed in 1-mm quartz/glass cuvettes. Femtosecond laser pulses were obtained from a conventional chirped pulse amplification system comprising of an oscillator (MaiTai, Spectra-Physics Inc.) that delivered ~80 fs pulses with a repetition rate of 82 MHz at 800 nm and a regenerative amplifier (Spitfire, Spectra Physics Inc.), which delivered 1 kHz amplified pulses of ~100 fs duration with an output energy of ~1 mJ. The bandwidth of the output was ~11 nm indicating nearly transform-limited pulses. Z-scan studies [24] were performed by focusing the 4-mm diameter input beam using an achromatic doublet (f = 120 mm). The peak intensities used in experiments were in the range of 150–1200 GWcm^{-2}. The entire studies were performed with solutions having concentrations of $\sim 5 \times 10^{-4}$ M providing 85–90% linear transmission at 800 nm. Similar peak intensities were maintained in the scans to ensure identical experimental conditions for both the samples. Closed aperture scans were performed at lower intensities to avoid contribution from the higher order nonlinear effects. The experiments were repeated more than once and the best data were used for obtaining the nonlinear optical coefficients from the best fits.

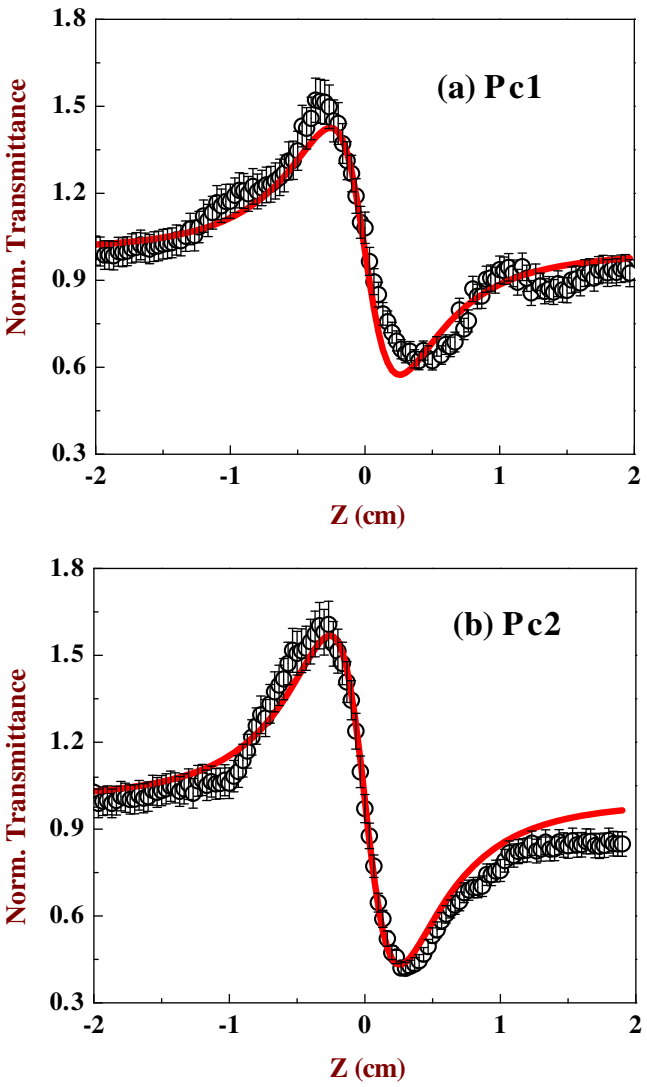

Fig. 1. Closed aperture Z-scan curves (open circles) for (a) Pc1 and (b) Pc2 obtained near 800 nm for a concentration of 5×10^{-4} M using an intensity of 2.5×10^{11} W/cm^2. Solid line is the theoretical fit.

3. Results and discussion

The fluorescence spectra of Pc1 (metal free) and Pc2 (Zn) obtained with pumping near 650 nm showed one emission peak close to 700 nm. The quantum yields for Pc1 and Pc2 were estimated to be ~0.65 and ~0.5, respectively. Fig. 1a and b illustrates the closed aperture Z-scan data recorded for Pc1 and Pc2 at an intensity of 2.5×10^{11} W/cm^2, well below the intensity levels leading to appreciable contribution from the solvent. Both the samples exhibited negative nonlinearity as discovered by the peak-valley signature. The magnitudes of the nonlinear refractive indices (n_2) evaluated, using the standard procedure, were $\sim 1.26 \times 10^{-13}$ esu (0.29×10^{-15} cm^2/W) for the free base phthalocyanine (Pc1) and $\sim 1.68 \times 10^{-13}$ esu (0.39×10^{-15} cm^2/W) for the zinc phthalocyanine (Pc2). It is evident that the metallic phthalocyanine has superior nonlinear refractive index value and this could be attributed to the presence of metal ion in the core. Earlier studies suggested the presence of heavy atom(s) within the phthalocyanine core to enhance the nonlinearities. The n_2 values obtained for these alkoxy phthalocyanines are comparable to those recorded with alkyl phthalocyanines which exhibited good figures of merit [9,10]. Open aperture Z-scan data of Pc1 and Pc2 indicated strong nonlinear absorption apparent from the changes in transmittance values. To assess the behavior of nonlinear absorption in Pc1 as a function of input intensity the open aperture scans were performed for four different peak intensities of (1) $I_1 = 1.5 \times 10^{11}$ W/cm^2, (2) $I_2 = 2.0 \times 10^{11}$ W/cm^2, (3) $I_3 = 3.7 \times 10^{11}$ W/cm^2, and (4) $I_4 = 5.1 \times 10^{11}$ W/cm^2. Fig. 2a–d shows the open aperture data recorded for Pc1. For intensities I_1, I_2, and I_3 the sample displayed RSA in SA with the RSA dip increasing. For higher intensities (I_4) the behavior switched from RSA in SA to SA in RSA. For Pc2 the four different intensities used in the study were (1) $I_1 = 1.5 \times 10^{11}$ W/cm^2, (2) $I_2 = 4.5 \times 10^{11}$ W/cm^2, (3) $I_3 = 8.0 \times 10^{11}$ W/cm^2, and (4) $I_4 = 12.1 \times 10^{11}$ W/cm^2. Fig. 3a–d shows the open aperture data recorded for Pc2. For intensities I_1 and I_2 the sample displayed pure SA. For higher intensities I_3 and I_4 the behavior switched from pure saturable type absorption to RSA in SA. For higher intensities the behavior was complex with switching of RSA to SA. We tried to understand this complex behavior through theoretical modeling considering a three-level system for these types of molecules interacting with ultrashort pulses. The femtosecond pulses used justify the usage of three-level model ignoring the triplet states since the intersystem crossing rates are much slower (typically few hundred picoseconds). A typical three-level energy diagram used for modeling is described in Fig. 4, where all the vibrational and rotational states of the first excited singlet state are denoted as S_1 and all

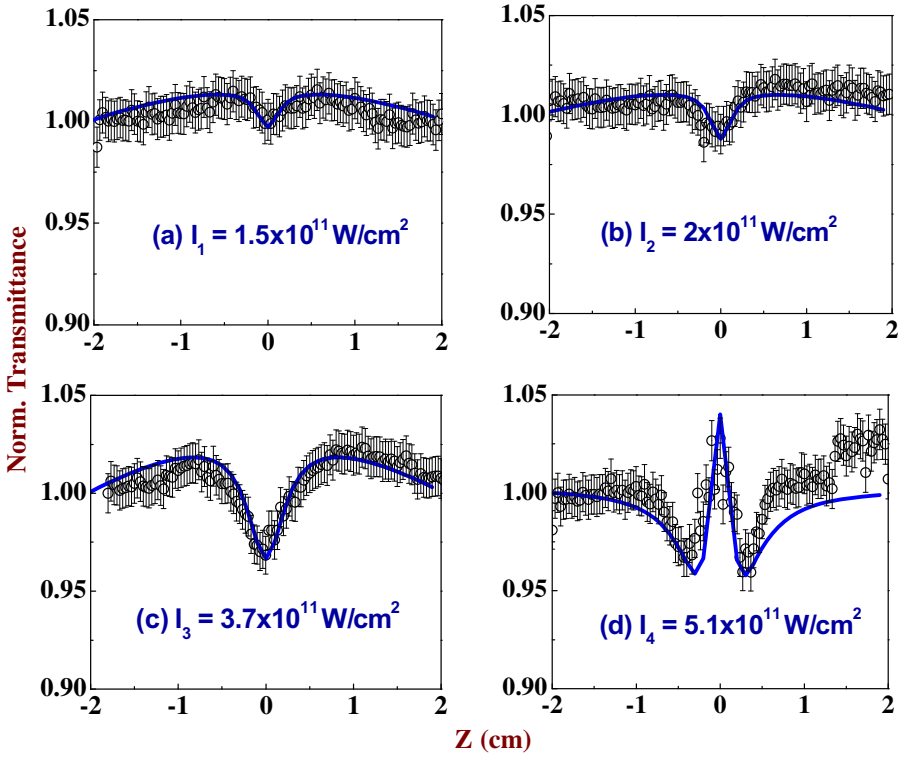

Fig. 2. (a–d) Open aperture Z-scan curves (open circles) obtained for Pc1 with varying input intensities.

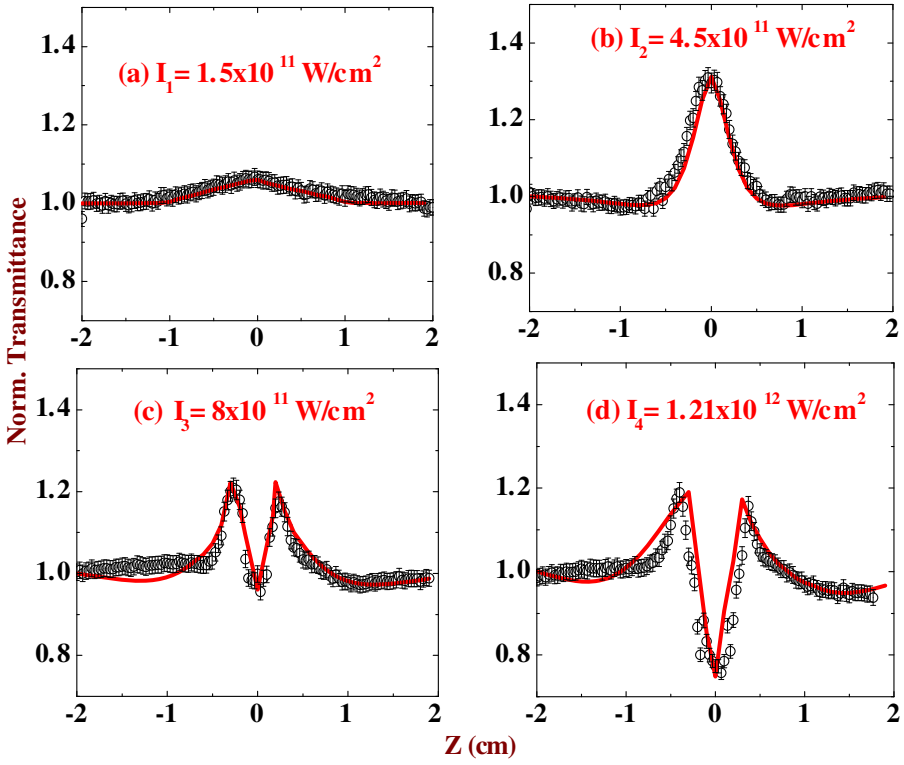

Fig. 3. (a–d) Open aperture Z-scan curves obtained for Pc2 with varying input intensities.

the excited states above the S_1 states are considered as S_n states. Eqs. (1)–(4) illustrate the processes leading to nonlinear absorption in phthalocyanine molecules with singlet states S_0, S_1, and S_n. For achieving better fits and the sake of completeness we have incorporated all nonlinear absorption mechanisms possible with femtosecond excitation in the rate equations: (a) excited state absorption (σ_1), (b) instantaneous two-photon absorption (β), and (c) three-photon absorption (γ). The contributions of different

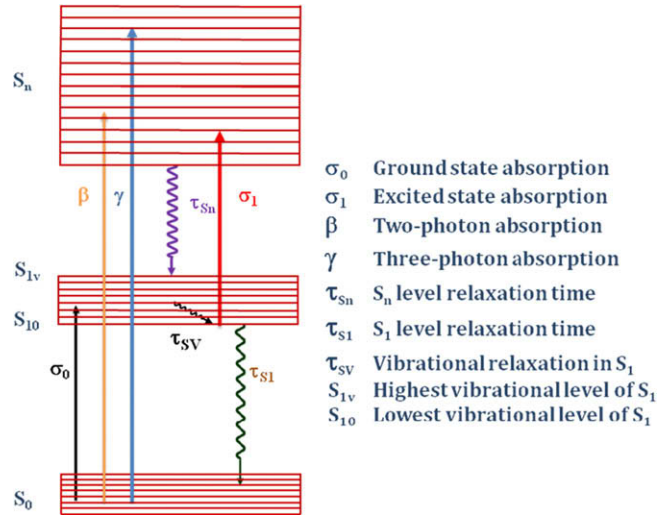

Fig. 4. Schematic energy level diagram for a chromophore with a singlet ground state.

nonlinear optical processes leading to SA in RSA or RSA in SA were found with numerical solution of the rate equations governing the population in the three levels.

$$\frac{dN_0}{dt} = -\frac{\sigma_0 I N_0}{\hbar\omega} - \frac{\beta I^2}{2\hbar\omega} - \frac{\gamma I^3}{3\hbar\omega} + \frac{N_1}{\tau_{s1}} \quad (1)$$

$$\frac{dN_1}{dt} = \frac{\sigma_0 I N_0}{\hbar\omega} - \frac{\sigma_1 I N_1}{\hbar\omega} - \frac{N_1}{\tau_{s1}} + \frac{N_2}{\tau_{sn}} \quad (2)$$

$$\frac{dN_2}{dt} = \frac{\sigma_1 I N_1}{\hbar\omega} + \frac{\beta I^2}{2\hbar\omega} + \frac{\gamma I^3}{3\hbar\omega} - \frac{N_2}{\tau_{sn}} \quad (3)$$

and the intensity transmitted through the sample is determined by

$$\frac{dI}{dz} = -\sigma_0 I N_0 - \sigma_1 I N_1 - \beta I^2 - \gamma I^3 \quad (4)$$

with

$$I = I_{00} \times \left(\frac{\omega_0^2}{\omega^2(z)}\right) \times \exp\left(-\frac{-t^2}{\tau_p^2}\right) \times \exp\left(-\frac{2^* r^2}{\omega^2(z)}\right)$$

and

$$\omega(z) = \omega_0 \left\{1 + \left(\frac{z}{z_0}\right)^2\right\}^{\frac{1}{2}}; \quad z_0 = \frac{\pi \times \omega_0^2}{\lambda}$$

σ_0 is the ground state absorption cross-section, σ_1 is the excited state absorption cross-section from S_1 and S_n *states, respectively,* β is the two-photon coefficient, γ is the three-photon coefficient, N_0, N_1, and N_2 are the population number densities in S_0, S_1, and S_n states, respectively. τ_{s1} and τ_{sn} are the lifetimes of the excited states S_1 and S_n, respectively. z_0 is the Rayleigh range, ω_0 is the beam waist at focus, τ_p is the input pulse width used, I is intensity as a function of r, t, and z. I_{00} is peak intensity at focus of the Gaussian beam. The differential equations were first de-coupled and then integrated over time, length, and along the radial direction before solving them numerically using Runge-Kutta fourth order method [26]. Assuming the input beam to be a Gaussian, the limits of integration for r, t, and z are varied from 0 to ∞, $-\infty$ to ∞, and 0 to L (length of the sample), respectively. Typical number of slices used for r, t, and z *was* 60, 30, and 5, respectively. σ_1, β, and γ are then estimated through least square fit of the experimental data. Lifetimes for these molecules were established from the fluorescence decay curves, presented in Fig. 5, and were utilized for theoretical fits of the open aperture data. The curve for Pc1 (Fig. 5a) exhibited a double exponential with two lifetimes of ~14 ns (>80% weight) and ~3.4 ns (<20% weight). We had utilized only the longer lifetime for the fittings with 100 fs pulse excitation since inclusion of both the lifetimes did not affect the fitted data significantly. Pc2 had a single exponential decay with ~3.4 ns life time. Better fits (smaller values of χ^2) were obtained when contribution from both 2PA and 3PA was included in the rate equations. The error bars indicated in Figs. 1–3 are indicative of some inaccuracies in the data collection. We also expect errors in fitting procedures, calibration of the intensity cut-off filters used, estimation of the focal spot size, and peak intensities. We anticipate the maximum error resulting from such factors in the evaluated values of nonlinear coefficients to be ~15%.

The multifaceted open aperture data obtained for Pc1 and Pc2, presented in Figs. 2 and 3, can be qualitatively explained as follows. Pc1 has lower ground state absorption cross-section ($\sigma_0 = 0.183 \times 10^{-18}\text{cm}^2$), compared to Pc2, indicating slow saturation of the first excited singlet state at lower intensities beyond which the nonlinear absorption takes over at higher intensities when the sample is scanned across the focus. For low pump intensities (I_1, I_2, and to an extent I_3) we see RSA in SA type of performance and for

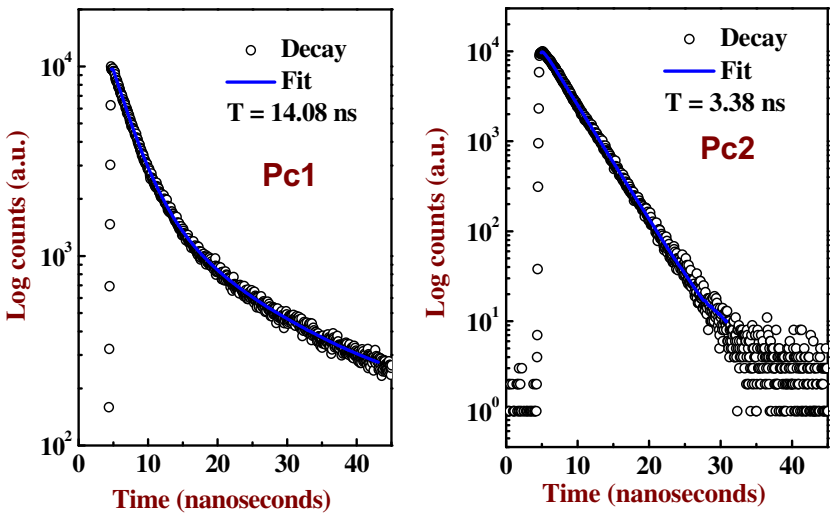

Fig. 5. Fluorescence decay data (open circles) of Pc1 and Pc2 dissolved in chloroform. Solid lines are the best fits. The decay time presented is the major component of the fits.

Table 1
Two-photon absorption coefficient (β), linear absorption cross-section (σ_0), excited state absorption cross-section (σ_1), nonlinear refractive index (n_2), and excited states lifetimes of the phthalocyanines excited with 800 nm, ~100 fs pulses

Sample	β ($\times 10^{12}$ cm W^{-1})	γ ($\times 10^{23}$ cm^3 W^{-2})	σ_0 ($\times 10^{18}$ cm^2)	σ_1 ($\times 10^{18}$ cm^2)	σ_1/σ_0	n_2 ($\times 10^{13}$ esu)	τ_1 (ns)
Pc1	1.5	0.8	0.183	2.4	13.1	-1.26 0.29×10^{-15} (cm^2/W)	14.0
Pc2	0.92	3.6	1.33	1.2	0.90	-1.68 0.39×10^{-15} (cm^2/W)	3.38
2(3), 9(10), 16(17), 23(24) Tetra *tert*-butyl phthalocyanine	–	9.1	–	–	–	0.56×10^{-15} (cm^2/W)	6.31
2(3), 9(10), 16(17), 23(24) Tetra *tert*-butyl zinc phthalocyanine	–	9.5	–	–	–	1.14×10^{-15} (cm^2/W)	3.18

very high input peak intensity (I_4) we observed RSA behavior even at places far from focus followed by saturation within the RSA near to the focus. We expect this saturation from the S_n excited states. The nonlinear coefficients for Pc1 were obtained from the fits to the experimental data (open circles are experimental data and the solid line is the fit in Fig. 3). The high value of σ_1, compared to σ_0, was 2.4×10^{-18}cm^2 which is anticipated since the S_1 life time value measured and used in the fits was ~14 ns. The value of 2PA (β) coefficient estimated was 1.5×10^{-12} cm W^{-1} (two-photon cross-section $\sigma_2 = 1.24 \times 10^{-48}$ cm^4 s/photon-molecule) and the 3PA (γ) coefficient was 0.8×10^{-23} cm^3 W^{-2} (three-photon cross-section $\sigma_3 = 1.64 \times 10^{-78}$ cm^6 s^2/photon^2-molecule). It is evident that excited state absorption (σ_1) is dominant compared to β and γ.

Pc2 has relatively higher ground state absorption cross-section ($\sigma_0 = 1.33 \times 10^{-18}$cm^2) and the life time of the S_1 state is considerably reduced to 3 ns due to quenching of the fluorescence. Saturation of the S_1 state is evident (Fig. 3a and b) at lower intensities with linear absorption being the responsible mechanism. However, for very high intensities RSA dons the dominating role and therefore we notice a dip in the SA behavior. The value of 2PA (β) coefficient estimated was 0.76×10^{-12} cm W^{-1} ($\sigma_2 = 0.76 \times 10^{-48}$ cm^{4}s/photon-molecule) and 3PA (γ) coefficient was 3.6×10^{-23} cm^3 W^{-2} ($\sigma_3 = 7.38 \times 10^{-78}$ cm^{6}s^2/photon^2-molecule). The value of σ_1 extracted from the fits was 1.2×10^{-18}cm^2 suggesting that its contribution is insignificant. The presence of nonlinear absorption is manifested at intensities closer to the focus as seen in Fig. 3c and d. This can be explained as 3PA and 2PA are intensity dependent processes (with I^3 and I^2 dependence) and will take over only at high peak intensities unlike σ_1 which has linear dependence on the intensity. For the case of Pc1, σ_1 has strong contribution to the nonlinear absorption and it shows up at intensities far from focus too which is apparent in Fig. 2d. The 3PA coefficient obtained for Pc2 compares very well with the values obtained for alkyl phthalocyanines reported recently by our group [9,10]. The cross-sections, however, differ by a normalization factor of 10^{-3} missing in those calculations. The data presented here for both Pc1 and Pc2 were obtained with solutions of concentration of $\sim 5 \times 10^{-4}$ M. The nonlinear absorption coefficients obtained for Pc1 and Pc2 from the theoretical fits are compiled in Table 1. The table also includes the data obtained for alkyl phthalocyanines for which we observed only three-photon absorption. However, the concentration we used in that case was a bit lower than the once used here. We noticed that the nonlinear absorption in these types of molecules is highly complicated and alters easily with different concentrations of the solutions and the peak intensities used. By choosing an appropriate concentration and intensity one can switch from a SA type of behavior to RSA and vice versa. A recent report by Gu et al. [27] has theoretical investigation of effective four-photon absorption where they proposed a two-step model of three-photon induced excited-state absorption, especially for poly-atomic molecules. This only proves the complexity of the nonlinear absorption process in these materials depending critically on the pulse duration, wavelength, absorption, and the concentration of the investigating species.

4. Conclusions

We have investigated the nonlinear optical properties of two alkoxy phthalocyanines at 800 nm with ultrashort pulses. Both these phthalocyanines possess strong n_2 and nonlinear absorption coefficients. Magnitudes of n_2 evaluated were $\sim 1.26 \times 10^{-13}$ esu for Pc1 and $\sim 1.68 \times 10^{-13}$ esu for Pc2. Open aperture Z-scan studies demonstrated complex behavior with switching over from SA to RSA and vice versa. Two-photon absorption, three-photon absorption, and excited state absorption were found to be responsible for the nonlinear absorption in these phthalocyanines.

Acknowledgments

S. Venugopal Rao and D. Narayana Rao acknowledge the financial support received from Department of Science and Technology (DST), India. Partial funding has been from a fast track DST project (SR/FTP/PS-12/2005).

References

[1] L.W. Tutt, T.F. Boggess, Prog. Quant. Electron. 17 (1993) 299.
[2] M. Calvete, G.Y. Yang, M. Hanack, Synth. Met. 141 (2004) 231.
[3] A. Slodek, D. Wohrle, J.J. Doyle, W. Blau, Macromol. Symp. 235 (2006) 9.
[4] M. Hanack, T. Schneider, M. Barthel, J.S. Shirk, S.R. Flom, R.G.S. Pong, Coord. Chem. Rev. 219–221 (2001) 235.
[5] G. de la Torre, P. Vazquez, F. Agullo-Lopez, T. Torres, Chem. Rev. 104 (2004) 3723.
[6] Y. Chen, M. Hanack, Y. Araki, O. Ito, Chem. Soc. Rev. 34 (6) (2005) 517.
[7] M.O. Senge, M. Fazekas, E.G.A. Notaras, W.J. Blau, M. Zawadzka, O.B. Locos, E.M. Ni Mhuircheartaigh, Adv. Mater. 19 (2007) 2737.
[8] J.J. Doyle et al., J. Opt. A: Pure Appl. Opt. 10 (2008) 075101.
[9] R.S.S. Kumar, S. Venugopal Rao, L. Giribabu, D. Narayana Rao, Proc. SPIE 6875 (2008). 68751D-1.
[10] R.S.S. Kumar, S. Venugopal Rao, L. Giribabu, D. Narayana Rao, Chem. Phys. Lett. 447 (2007) 274.
[11] N. Venkatram, L. Giribabu, D. Narayana Rao, S. Venugopal Rao, Appl. Phys. B 91 (2008) 149.
[12] S.J. Mathews, S. Chaitanya Kumar, L. Giribabu, S. Venugopal Rao, Opt. Commun. 280 (1) (2007) 206.
[13] S.J. Mathews, S. Chaitanya Kumar, L. Giribabu, S. Venugopal Rao, Mat. Lett. 61 (22) (2007) 4426.
[14] S. Venugopal Rao, N.K.M.N. Srinivas, L. Giribabu, B.G. Maiya, D. Narayana Rao, R. Philip, G. Ravindra Kumar, Opt. Commun. 182 (2000) 255.
[15] D. Narayana Rao, S. Venugopal Rao, F.J. Aranda, M. Nakashima, J.A. Akkara, J. Opt. Soc. Am. B 14 (10) (1997) 2710.
[16] E.M. Garcia-Frutos, S.M. O'Flaherty, E.M. Maya, G. de la Torre, W. Blau, P. Vazquez, T. Torres, J. Mater. Chem. 13 (2003) 749.
[17] H. Bertagnolli et al., J. Mater. Chem. 15 (2005) 683.
[18] A. Auger et al., J. Mater. Chem. 13 (2003) 1042.
[19] W. Sun, G. Wang, Y. Li, M.J.F. Calvete, D. Dini, M. Hanack, J. Phys. Chem. A. 111 (2007) 3263.
[20] Y. Chen, N. He, J.J. Doyle, Y. Liu, X. Zhuang, W.J. Blau, J. Photochem. Photobiol. A: Chem. 189 (2007) 414.
[21] S. Vagin, M. Barthel, D. Dini, M. Hanack, Inorg. Chem. 42 (8) (2003) 2683.
[22] G. He, L.-S. Tan, Q. Zheng, P.N. Prasad, Chem. Rev. 108 (4) (2008) 1245.
[23] E. Hernández, S. Yang, E.W. Van Stryland, D.J. Hagan, Opt. Lett. 25 (2000) 1180.
[24] M. Sheik-Bahae, A.A. Said, T. Wei, D.J. Hagan, E.W. Van Stryland, IEEE J. Quant. Electron. 26 (1990) 760.
[25] C.C. Leznoff, A.B.P. Lever (Eds.), Phthalocyanines Properties and Applications, Wiley VCH Publishers, New York, 1993.
[26] S. Venugopal Rao, D. Narayana Rao, J.A. Akkara, B.S. DeCristofano, D.V.G.L.N. Rao, Chem. Phys. Lett. 297 (1998) 491.
[27] B. Gu, W. Ji, Opt. Exp. 16 (14) (2008) 10208. and references therein.